On Hydrophobic and Icephobic Properties of TiO$_2$-Doped Silicon Rubber Coatings

Faranak Arianpour, Masoud Farzaneh

NSERC/Hydro-Quebec Industrial Chair and Canada Research Chair on Atmospheric Icing of Power Network Equipment (CIGELE/INGIVRE),
Department of Applied SciencesUniversité du Québec à Chicoutimi,
555 University boulevard, Saguenay, PQ, Canada G7H 2B1
faranak.arianpour@uqac.ca; masoud_farzaneh@uqac.ca

Abstract- *In the present work, flat and micro-/nano-rough water and ice-repellent coatings based on room-temperature vulcanized silicone rubber (RTV SR) incorporated with titania (TiO$_2$) nanopowder as a dopant were prepared and investigated. Such water and ice-repellent coatings are potential candidates for protecting high-voltage equipment such as conductors and insulators. Supehydrophobic samples with contact angle (CA) >145° and contact angle hysteresis (CAH) ~5-10° were prepared by spin coating TiO$_2$-loaded RTV SR suspensions on etched substrates. The SEM investigations of the sample surfaces revealed that the alumina filler (loaded into the as-supplied silicone rubber product) had some influence on the surface topographies of the prepared coatings. It was also found that the nanopowders used as dopants further increased the surface roughness (and correspondingly - water repellency) of the coatings. While the TiO$_2$-doped RTV SR demonstrates high CA and low CAH values, which is characteristic of the Cassie wetting regime, the wetting mode on the rough RTV SR coated sample with high CAH is expected to be a mixed Cassie-Wenzel regime. The anti-icing behaviour of the coating was studied under atmospheric icing conditions. Rough superhydrophobic coatings prepared with TiO$_2$ nanoparticles of dielectric constant (~80) resulted in reducing the ice adhesion strength by at least ~7 times compared to a mirror-polished aluminium sample and by ~9 times compared to an as-received aluminium sample. At approximately -15 ^{o}C, water droplets were found to freeze on polished aluminium after approximately 5 s, while their freezing was delayed by as long as ~12-13 min on a superhydrophobic nanocomposite surface doped with TiO$_2$ powder. This delay is explained by the insulating properties of the rough surface that entraps a significant amount of air into its structure. Therefore, the coatings prepared show promise for industrial applications on high-voltage equipment, including insulators, since they can reduce ice accumulation, while also reducing the risk of flashover on outdoor insulators.*

Keywords: Room-temperature Vulcanized Silicone Rubber (RTV SR), Titania (TiO$_2$), Hydrophobicity and Superhydrophobic, Water and Ice Repellency, Insulator, Dielectric Constant, Ice Adhesion Strength, Flashover

1. Introduction

Atmospheric ice is formed on overhead transmission and distribution lines when they are exposed to supercooled water droplets or snow particles. This may lead to serious risk to the security of overhead networks (Farzaneh and Melo, 1994, Farzaneh, 2008, Farzaneh, 2009, Farzaneh and Chisholm, 2009). Ice accretion, together with superimposed contamination, is well-known to cause a decrease in the electrical performance of outdoor insulators, sometimes resulting in outages (Farzaneh and Chisholm, 2009). Ice or wet-snow can cause severe trouble due to their high adherence to both metallic and insulating surfaces. Prevention of ice accretion on surfaces requires reduction of ice adhesion strength. Thus, various anti-icing and de-icing techniques, e.g. chemical, thermal or mechanical removal of ice build-ups, have been developed for decades. Although the majority of the techniques currently in use are called active de-icing techniques, all of them are employed where ice accumulations are already considerable. Developing passive anti-icing or ice-phobic coatings is gaining in popularity.

These kinds of coatings prevent or hinder ice and wet-snow accumulation on such surfaces and are believed to provide reduced ice adhesion (Farzaneh and Chisholm, 2009). Although chemical, thermal and mechanical de-icing techniques are usually applied to mitigate icing effects, however, these methods are not always advantageous due to time and high cost involved as well as their limited rather than general application. An alternative way to prevent ice accretion on high-voltage equipment would be to apply coatings with ice-repellent properties (Farzaneh and Melo, 1994, Laforte *et al.*, 1998, Petrenko and Peng, 2003). Recently, several coatings for ice-phobic application have been tested and reported but the best results belonged to greases and lubricants and not to solid coatings (Laforte *et al,* 2005, Wong *et al.,* 2011, Smith *et al.,* 2013). These ice-phobic coatings must necessarily fulfil both of the following requirements for a true solution: first, they must efficiently reduce snow or ice adhesion, and second, they must have a reasonably long service-life or durability. In this regards, polymers with low critical surface tension such as organopolysiloxane and tetrafluoroethylene (Teflon®) were examined. Those coatings exhibited satisfactory traction on wet roads; they produced very low run-off water contamination and thus demonstrated a significant reduction in ice adhesion (Croutch *et al*, 1992). An additional series of investigation revealed that fluorinated and polysiloxane coated surfaces had the poorest wetting by water and are good candidates for ice-phobic coatings (Croutch *et al*, 1992). Although deicing fluids can be applied to ice-covered structures to eliminate such ice build-ups, these substances can have significant negative environmental impacts and thus can only be used as requires a large supply of energy. Electrolysis is another approach found to be effective for removing ice from certain surfaces; however, it is not still a practical method (Petrenko *et al*, 1999). Silicone rubber (RTV SR) coated high-voltage insulators are sometimes preferred to conventional porcelain insulators because of the hydrophobic properties of their surface, light weight and easy handling. That is why they are good candidates to be used in highly polluted regions (Cherney, 2005). In recent years, nanoparticles incorporated polymer nanocomposites have been widely studied for their potential application for improving the electrical performance of high-voltage insulators (Cherney, 2005, Li *et al*., 2006, Jana *et al*., 2007, Choi *et al*., 2007, Ma *et al*., 2008, Kobayashi *et al*., 2008). Among the various coatings considered, semiconductive ones, including polymers incorporating nanoparticles, have been considered for that purpose (Cherney, 2005, Liao *et al.,* 2007, Siderakis and Agoris, 2008, Rastegar and Ranjbar, 2008, Kobayashi *et al.,* 2008, Farzaneh and Chisholm, 2009). While previous work was mainly focused on the electrical and mechanical properties of nanoparticles-incorporated RTV SR coatings, in this study aims at achieving a better understanding of the ice-repellent properties of TiO$_2$-doped silicon rubber in view of its application to outdoor insulators.

2. Experimental Procedure

TiO$_2$ nanopowder with particle size below 100 nm, from Sigma-Aldrich, has been used to both modify the electrical performance of the RTV SR layer enhancing its superhydrophobic properties through adding macro/nano-scale roughness. It should be noted that the RTV SR product (used as-supplied from the manufacturer) had alumina micro- particles (average size ~3 µm) as a filler improving its mechanical properties. However, since the concentration of such alumina particles was constant, their contribution to the properties of the tested samples was same for both non-doped and doped (with TiO$_2$ powders) coatings. Therefore, adding different amounts of the above dopant nanopowder allowed us to elucidate their effect on the hydrophobic and ice-releasing properties of doped coatings in comparison with their non-doped counterparts. The coatings were prepared using a spin-coater from Laurel (WS-400B-6NPP) followed by curing in a conventional oven in air. The choice of metal substrates was mainly dictated by the necessity to use some samples for icing/de-icing experiments in a centrifuge. Aluminium alloy (AA6061) was used as substrate. The influence of different parameters on the formation and properties of such layers has been analyzed in order to optimize the coating process. The RTV silicon rubber (Dow Corning, HVIC 1547) was mixed with n-hexane. Then, the TiO$_2$ nanoparticles were added under vigorous magnetic agitation. After careful stirring, the suspension was used to prepare nanoparticles-incorporated coatings on Al samples etched with diluted hydrochloric acid, HCl. In parallel, undoped RTV was coated on a flat substrate for comparison. The samples were coated by using a spin-coater whose spinning rate was set at 500 rpm and 3000 rpm for the first and second stages, respectively. Upon coating, all samples were heat-treated at 80 °C in air overnight to remove residual solvents.

The wetting behaviour of the coatings was assessed by the water contact angle (CA), measured on a Krüss DSA100 contact-angle goniometer following standard procedures. These were measured by the sessile-drop method: small water droplets (4µl in volume) were gently placed on the surface, and their shape was evaluated by using the goniometer optics and software. The CA values reported here are the averages of at least five measurements on various parts of each sample. They were recorded at 23±0.5 °C. Scanning electron microscopy (SEM) was used to take surface images of the coatings, and thus reveal their surface topography. Surface roughness characterization of prepared samples was performed using an optical profilometer CHR450 from STIL. Ice adhesion strength was evaluated using a custom-made centrifuge apparatus (centrifuge adhesion testing machine) placed in a cold room at subzero temperature. The type of ice used was glaze ice, prepared by spraying supercooled micrometer-sized water droplets (~80 µm) in a wind tunnel at -10 °C, at wind speed of 11 m.s^{-1} and water feed rate of 2.5 g.m^{-3}. The process of ice preparation

has been before described in greater detail somewhere else (Kulinich and Farzaneh, 2009, Jafari *et al.*, 2010, Kulinich and Farzaneh, 2011, Farhadi *et al.,* 2011, Kulinich *et al.*, 2011).

Table 1 presents the contact angle (CA) and contact angle hysteresis (CAH) for the different samples. The samples prepared in this study were: polished Al (sample 1), RTV SR coated polished Al (sample 2), HCl etched (rough) RTV SR coated Al (sample 3) and rough RTV silicon rubber coated sample with TiO_2 nanopowders incorporated (sample 4).

Table. 1. CA, CAH and freezing times of different samples.

Sample	1	2	3	4
Topography	Polished Al	RTV SR flat	RTV SR rough	RTV SR rough
Filler	-	-	-	TiO_2
CA (deg.)	55 ± 5	102 ± 2	143±1.5	146 ± 1
CAH (deg.)	≥ 50	45	40	5
Freezing Times (s)	3/5	85/218	37/347	705/735

3. Results and Discussion

Figure 1 shows that by changing the RTV silicon rubber /hexane ratio from 1:1 to 1:4, the samples prepared by spin coating RTV silicon rubber suspensions with 1 wt. % of TiO_2 showed contact angle values gradually increasing with the RTV silicon rubber dilution degree. At the same time, contact angle hysteresis values of the samples decreased as low as ~5-10°, which is characteristic of superhydrophobic state. Therefore, supehydrophobic samples with contact angle value of >145° and contact angle hysteresis of ~5-10° could be prepared by spin coating TiO_2-loaded RTV silicon rubber suspensions on etched substrates. Figure 1b shows that water droplets can move on such surfaces without any significant distortion, which is characteristic of low contact angle hysteresis values. As it is evident in figure 1, obvious significant increase in the contact angle values of the samples was obtained when the prepared suspensions were diluted three or four times. Significant decrease by 10 to 20° was also observed in the obtained contact angle hysteresis values. This can be explained by better filling of valleys between surface asperities (on rough substrates) by thinner suspensions during spin coating. As a result, rough surfaces with asperities well covered with RTV silicon rubber and deeper valleys were produced, which are wetted in the Cassie-Baxter mode (i.e. with high contact angle and low contact angle hysteresis values).
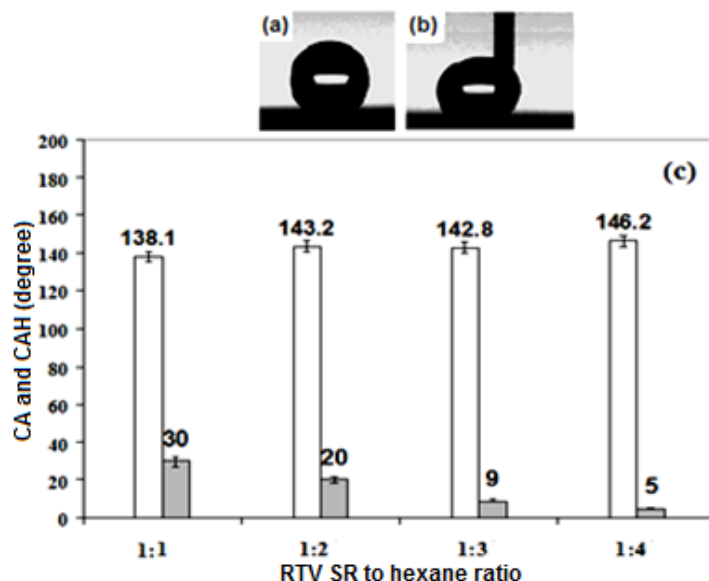

Fig. 1. (a) Water contact angle (CA) and (b) water contact angle hysteresis (CAH) of coating prepared by spin coating hexane dilution of RTV SR (1:4) with 1 wt.% TiO_2 nanoparticles incorporated, (c) contact angle and CAH as a function of RTV SR/hexane ratio with 1 wt.% of TiO_2 nanoparticles incorporated.

Figure 2 shows SEM images of the etched Al samples coated with RTV SR (a), and RTV SR/TiO_2 (b).
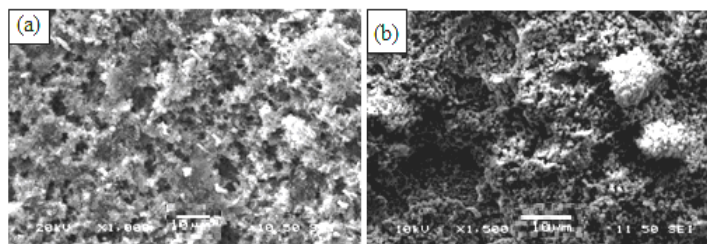

Fig. 2. SEM surface images of (a) etched Al sample coated with RTV SR, (b) etched Al sample coated with RTV SR /TiO_2 (1 wt. %).

Scanning electron microscopy (SEM) images from etched aluminium sample coated with RTV silicon rubber/hexane (1:4 v/v) and RTV SR/TiO_2 are shown in Figure 2. Based on the SEM images obtained from different prepared coatings in this research work, dissimilar surface topographies were observed. This variation in surface topography caused different coating properties. It is well seen in figure 2a that the alumina filler particles (which are a part of the as-supplied silicone rubber product used in this study) contributed to the topographies of the prepared coatings. Such micro-sized particles are seen in both Figs. 2a and 2b. Though TiO_2 noparticles are relatively small, and therefore difficult to be seen in Fig. 2b, they definitely contributed to both surface roughness and water-repellent properties of rough titania-doped RTV silicon rubber coatings. More specifically, while the non-doped rough sample in Fig. 2a demonstrated CAH value of ~40°, its titania doped

counterparts (in Fig. 1c) exhibited improved CA value of ~146° and decreased CAH value of ~5°, (see Fig. 1c). This effect can be easily explained by the nano-roughness added by nano-sized TiO_2 particles, which could further improve the water repellency of the doped RTV silicon rubber coatings compared with that of the non-doped rough sample in Fig. 2b. Also, another prove to the mentioned explanation and to account for the different surface roughness of these two samples, Fig. 3 presents their surface parameters measured by means of optical profilometry, i.e. root-mean-square roughness (Sq) which represents the standard deviation of the surface profile from its mean value.
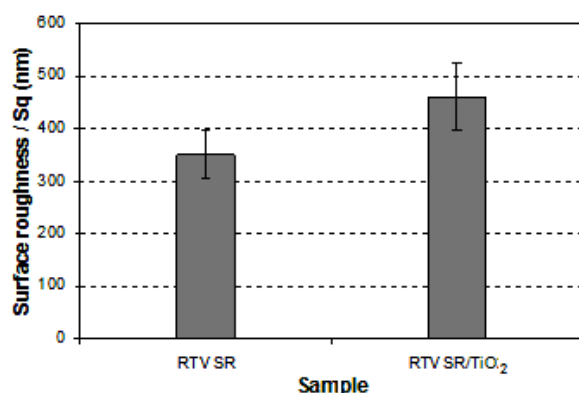

Fig. 3. Surface roughness (root-mean square) of etched Al samples coated with RTV SR and RTV SR /TiO_2 (1 wt. %).

Figure 4 shows images of water droplets moving along the surface of rough samples coated with TiO_2-doped RTV silicon rubber (a) and rough RTV SR-coated sample (b) showing low and high CAH values, respectively. Both samples had the same chemistry as they are covered with RTV silicon rubber as top layer. However, their topographies are somewhat different, leading to different wetting regime on these surfaces.
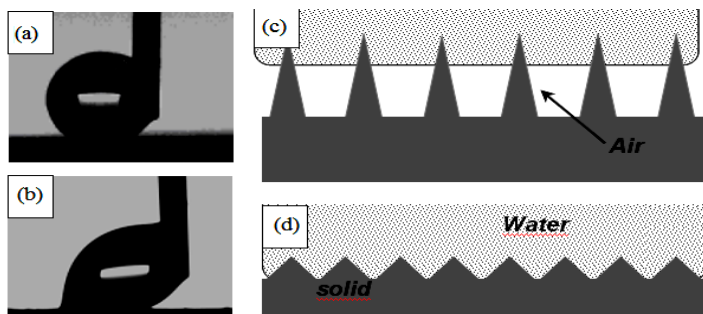

Fig. 4. Shape of a water droplet on superhydrophobic sample RTV SR/ TiO_2 (a) and on a rough RTV SR-coated surface (b); Cassie model (c) and Wenzel model (d).

While the TiO_2-doped RTV silicon rubber demonstrates high CA and low CAH values, which is characteristic of the Cassie wetting regime (Fig. 4c), the wetting mode on the

rough RTV SR coated sample with high CAH is expected to be a mixed Cassie-Wenzel regime (Fig. 4d). The water-solid contact areas on these samples are very different, being very small on the TiO_2-doped RTV SR sample and larger on the high-CAH sample which leads to the contrasting values of CAH observed in Figs. 4a, b. When the CAH value on the TiO_2-doped RTV SR was small, the sample was wetted in the Cassie mode, i.e. with a small water-solid contact area. Table 1 demonstrates that hydrophobic samples with different values of CA (from ~102° to ~147°) and CAH (from ~5° to ~45°) were prepared with varying coatings.

The shear stress of ice detachment value of the RTV SR coated sample with TiO_2 nanoparticles incorporated as a function of icing/de-icing cycles is shown in Fig. 5. Ice adhesion on as-received and mirror polished aluminium was measured under the same conditions, and the results are also presented in Fig. 5. For the RTV SR/ TiO_2 coating considered, the sample was subjected to 10 successive icing/de-icing operations. As-received uncoated flat aluminium was used as a standard showing ice detachment shear stress of 445±20 kPa. The value of the mirror-polished aluminium surface (350±19 kPa) is also shown in Fig. 5. Shear stress of ice detachment on coated surface varied from 50 to 72 kPa for the coating spin-coated from RTV SR (1:4 v/v) solution with 1 wt. % of TiO_2 nanoparticles. Reduced ice adhesion can be related to the low surface energy coating on the sample and air incorporation into the rough surface structure. It was observed that value of ice adhesion strength was at least 7 times lower than that obtained for the mirror-polished Al sample and 9 times lower than that of the as-received aluminium sample.
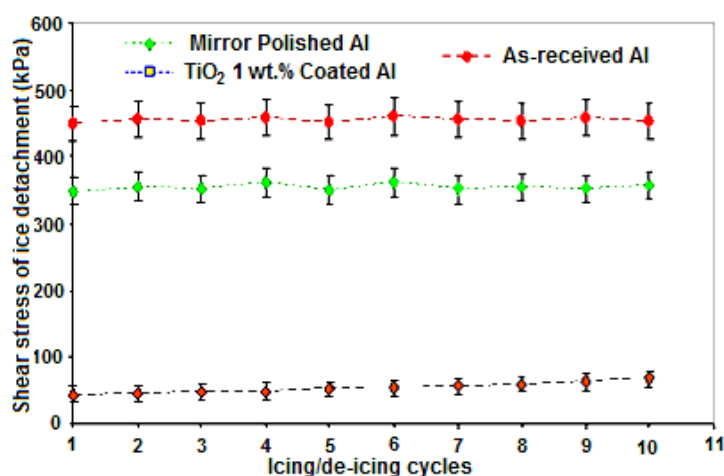

Fig. 5. Shear stress of ice detachment vs. icing/de-icing cycle number for as-received aluminium, mirror-polished aluminium, and coating prepared from RTV SR (1:4 v/v) solution with 1 wt. % of TiO_2 nanoparticles incorporated.

Good correlation between hydrophobicity of surfaces and their ice-repellent behaviour was previously reported by other research groups (Saito *et al.,* 1997, Petrenko and Peng,

2003, Kulinich *et al.,* 2009, Farhadi *et al.,* 2011). The adhesion reduction factor (*ARF*) values of the RTV SR/hexane volume ratio with 1 wt. % TiO_2 nanoparticles incorporated coated sample as a function of icing/de-icing cycles are presented in Fig. 6. The *ARF* values of the coating spin-coated from RTV SR/hexane (1:4 v/v) solution with 1 wt. % of TiO_2 nanoparticles incorporated decreased from 6.96 to 4.95, by increasing the number of icing/de-icing cycles to 10 times (Fig. 6).
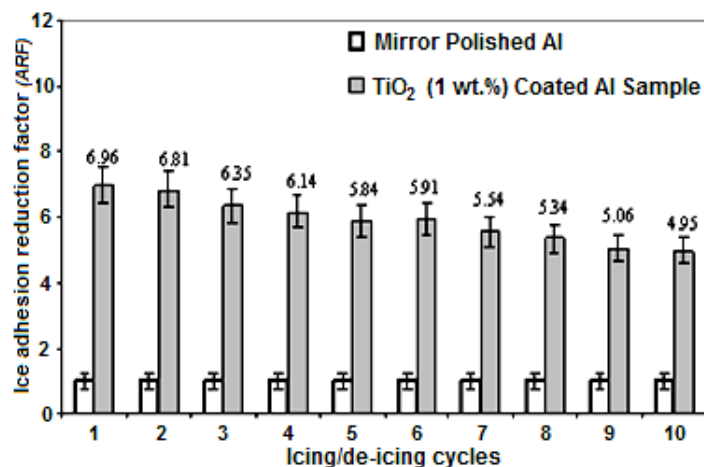

Fig. 6. Ice adhesion reduction factor (ARF) as a function of icing/de-icing cycles on mirror-polished Al and TiO₂-doped RTV SR coating.

However, a decrease in *ARF* values was observed after as many as 10 icing/de-icing events. This can be attributed to the gradual damage of the rough coatings during icing/de-icing cycles which caused the decrease of the superhydrophobic properties of the coated Al surface. However, its surface deteriorates during successive icing/deicing cycles can lead to ice mechanical anchoring since liquid water penetrates the porous surface (Farhadi *et al.*, 2011; Kulinich *et al.*, 2011; Chen *et al.*, 2012).

Figure 7 demonstrates freezing of 4-μL water droplets on four different surfaces: (a) polished Al, (b) flat RTV SR sample, (c) rough TiO₂-doped RTV SR. The images present droplet shapes and times (i) immediately after the droplets were placed on the cold surfaces, (ii) after water-solid interface ice nucleation, and (iii) after complete drop crystallization. Ice nucleation at the solid-water interface was observed and determined as the time when light intensity inside the droplet significantly changed (see Fig. 7). This nucleation occurred after ~3s on the flat uncoated Al, and after ~705s on the rough Al coated with RTV SR/TiO_2, respectively (see Fig. 7).
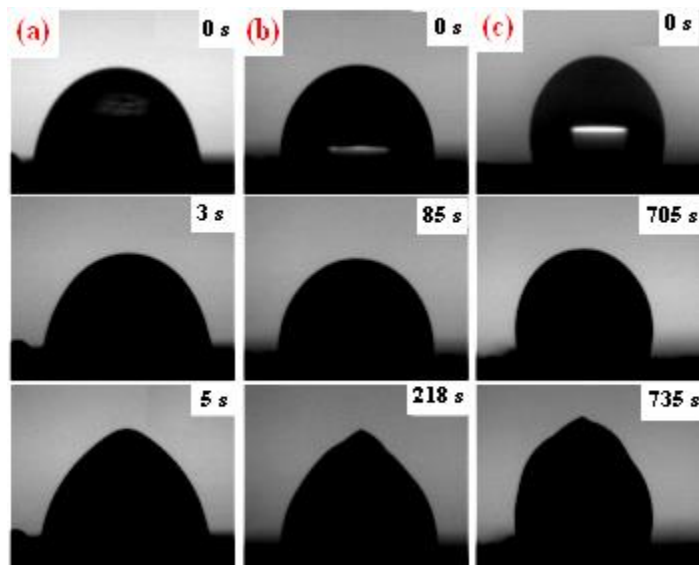

Fig. 7. Image sequences of water droplets freezing on polished Al (a), flat RTV SR surface (b), and, TiO₂-doped RTV SR surface (c). The images correspond to initial droplets (top), ice crystallization at the solid-water interface (middle), and full drop crystallization (bottom).

Figure 8 illustrates how heat is transferred in the water-solid interface area of a water droplet residing on a superhydrophobic surface (the Cassie regime). It is evident from this schematic model that the rougher a surface is, the lesser the water-solid contact area will be and the more entrapped air will be present in the water-solid interface. Therefore, the heat exchange process between water droplets and the solid will be reduced due to the entrapped air acting as an insulator, leading to longer and delayed freezing time of water droplets. Therefore, as seen in Fig. 6, water drops were frozen with a much longer delay on superhydrophobic samples (~12-13 min) compared to their flat or uncoated counterparts. However, it should be noted that the rough hydrophobic surface coated with RTV SR did not delay water freezing on its surface by much. This could be related to the larger water-solid contact area observed on this surface, which agrees well with the relatively large value of CAH observed on this surface (~ 40°).
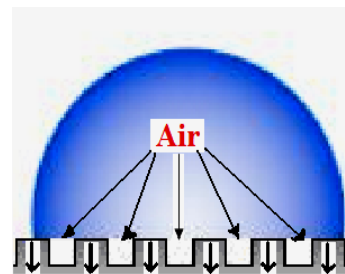

Fig. 8. Water drop on a superhydrophobic surface. Heat transfer at surface/ water drop interface is shown by the short arrows.

4. Conclusions

In this study, hydrophobic and ice-repellent behaviour of silicon rubber coatings doped with TiO_2 nanopowder was studied. For this purpose, flat and rough coatings were prepared, using TiO_2 nanopowder as a filler that is (or can be) used to modify both mechanical and electrical properties of silicone rubber layers on electric insulators. On rough (etched) substrates, coatings with both high values of CA and low values of CAH were prepared when TiO_2 nanopowder was incorporated. Hexane-diluted RTV SR suspensions were found to lead to coatings with improved water repellency. The SEM investigations of the sample surfaces revealed that the alumina filler (loaded into the as-supplied silicone rubber product) had some influence on the surface topographies of the prepared coatings. It was also found that the nanopowders used as dopants further increased the surface roughness (and correspondingly-water repellency) of the coatings. This result can be as well proved by different surface roughness values obtained for these two samples which measured via optical profilometry using root-mean-square roughness (Sq) values. Ice-releasing properties of superhydrophobic coatings were shown to be enhanced, if compared to those of flat coatings with same composition, which is explained by the reduced ice-solid contact areas on such surfaces. Ice-releasing performance of the coated samples showed some deterioration after 10 icing/de-icing cycles. RTV silicon rubber coating doped with TiO_2 nanopowder sample demonstrated initial ice adhesion strength values at least ~7 times lower than those obtained on the mirror-polished aluminium and ~9 times lower than those on the as-received uncoated Al sample. This decrease in ice adhesion strength can lead to easier removal of accumulated ice from such coated surfaces. Freezing of water droplets on polished Al, flat RTV SR surface, RTV SR/TiO_2 samples were investigated by placing droplets on surfaces at -15ºC. While on flat uncoated Al, small droplets froze after ~3-5 seconds, their freezing was significantly delayed on TiO_2 incorporated RTV SR (rough) coating, being ~12-13 min. The delayed freezing of water drops on the superhydrophobic surfaces prepared is explained by the reduced water-solid contact areas on such surfaces. As the water-surface interface on such samples trap a large extent of air, this slows down any heat exchange between water drops and cold surfaces, leading to significantly delayed water freezing. Taking into account the high water mobility observed on such surfaces (i.e. low CAH), this shows promise as water can be removed from such superhydrophobic surfaces before getting frozen. Thus, the RTV SR/TiO_2 coating prepared in this study show promise as both self-cleaning and anti-ice material which is expected to reduce flashover risks on high-voltage insulators.

Acknowledgements

References

Cherney, E. A, (2005), Silicone rubber dielectrics modified by inorganic fillers for outdoor high voltage insulation applications, IEEE Transactions on Dielectrics and Electrical Insulation, 12, 1108.

Chen, J., Liu, J., He, M., Li, K., Cui, D., Zhang, Q., Zeng, X., Zhang, Y., Wang, J., and Song, Y., (2012), Superhydrophobic surfaces cannot reduce ice adhesion, Applied Physics Letter, , 101, 111603.

Choi, S. H., Kim, I. D., Hong, J. M., Park, K. H., Oh, S. G., (2007), Effect of the dispersibility of BaTiO3 nanoparticles in BaTiO$_3$/polyimide composites on the dielectric properties, Material Letters, 61, 2478.

Croutch, V. K., Hartley, R. A. (1992). Adhesion of ice to coatings and the performance of ice release coatings, Journal of Coating Technology, 64, 41.

Farzaneh. M. (2008). Atmospheric Icing of Power Networks, Springer, Berlin, 381 p

Farzaneh, M. (2009), IEEE standard 1783 – guide for test methods and procedures to evaluate the electrical performance of insulators in freezing conditions. IEEE Press, New York.

Farzaneh, M., Chisholm, W. A. (2009). Insulators for icing and polluted environments, IEEE Press series on Power Engineering, IEEE/John Wiley, New York, 680 p.

Farzaneh, M., Melo. O. T., (1994), Flashover performance of insulators in the presence of short icicles, International Offshore and Polar Engingeering, 4, 112.

Farhadi, S., Farzaneh, M. and Kulinich, S. A. (2011), Anti-icing performance of superhydrophobic surfaces. Surface Science, 257, 6264.

Jana, S., Khojin, A.S., Zhong, W. H., Chen, H., Liu, X., Huo, Q., (2007), Effect of gold nanoparticles and lithium hexafluorophosphate on the electrical conductivity of PMMA, Solid State Ionics., 178, 1180.

Jafari, R., Menini, R., Farzaneh, M., (2010), Applied Surface Science 257, 1540.

Kobayashi, Y., Tanase, T., Tabata, T., Miwa, T. and Konno, M., (2008), Fabrication and dielectric properties of the BaTiO3-polymer nano-composite thin films, Journal of European Ceramic Society, 28, 117.

Kulinich, S. A., Farzaneh, M., (2009), Ice adhesion on super-hydrophobic surfaces, Applied Surface Science, 255, 8153.

Kulinich, S. A., Farzaneh, M., (2009), How Wetting Hysteresis Influences Ice Adhesion Strength on Superhydrophobic Surfaces, Langmuir, 25, 8854.

Kulinich, S. A., Farzaneh, M., (2010), On ice-releasing properties of rough hydrophobic coatings. Cold Regions Science and Technology, 65, 60.

Kulinich, S. A., Farhadi, S., Nose, K., Du, X. W., (2011), Superhydrophobic Surfaces: Are They Really Ice-Repellent?, Langmuir, 27, 25.

Laforte, C., Beisswenger, A. (2005). Icephobic material centrifuge adhesion test., in international workshop on atmospheric icing on structures (IWAIS), Montreal, Canada.

Laforte, J. L., Allaire, M. A., Laflamme, J., (1998), State-of-the-art on power line de-icing, Atmospheric Research, 46, 143.

Li, C., Gu, Y., Xiaobo, L., Yaobang, Z. and Anbing, T., (2006), Synthesis and dielectric property of polyarylene ether nitriles/titania hybrid films, Thin Solid Films., 515., 1872.

Liao, W. Y., Jia, Z.D., Guan, Z. C., Wang, L. M., Yang, J.,. Fan, J. B, Su, Z. Y. and Zhou, J. (2007), Reducing ice accumulation on insulators by applying semiconducting RTV silicone coating, IEEE Transactions on Dielectrics and Electrical Insulation, 14, 1446.

Ma, P.C., Tang, B.Z., Kim, J.K., (2008), Effect of GNT decoration with silver nanoparticles on electrical conductivity of GNT-polymer composites, Carbon., 46, 1497.

Petrenko, V. F., Peng, S., (2003), Reduction of ice adhesion to metal by using self-assembling monolayers (SAMs), Canadian Journal of Physics, 81, 387.

Petrenko, V. F., Qi, S. G. (1999). Reduction of ice adhesion to stainless steel by ice electrolysis, Journal of Applied Physics 86, 5450.

Rastegar, S. and Ranjbar, Z., (2008), DC and AC electrical conductivity of electro-deposited carbon-black-epoxy composite films, Progress in Organic Coatings, 63, 1.

Saito, H., Takai, K. and Yamauchi, G. (1997). Water- and ice-repellent coatings. Surface Coatings International, 80, 168.

Siderakis, K. and Agoris, P., (2008), Performance of RTV silicone rubber coatings installed in coastal systems, Journal of Electric Power Systems Research 78, 248.

Smith, J. D., Dhiman, R., Anand, S., Garduno, E. R., Cohen. R. E., McKinleya. G. H., Varanasi. K. K., (2013), Droplet mobility on lubricant-impregnated surfaces, Soft Matter, 9, 1772.

Wong, T. S., Kang. S. H,, Tang. S. K. Y., Smythe. E. J., Hatton. B. D., Grinthal. A., Aizenberg. J., (2011), Bioinspired self-repairing slippery surfaces with pressure-stable omniphobicity, Nature Letter, 477, 443.

Yang, B. Y., Montgomery, R. (2003). De-icers derived from corn steep water, Journal of Biotechnology, 90, 265.